

1 **Bayesian assessment of chlorofluorocarbon (CFC), hydrochlorofluorocarbon (HCFC) and**
2 **halon banks suggest large reservoirs still present in old equipment**

3
4 Megan Lickley¹, John Daniel², Eric Fleming^{3,4}, Stefan Reimann⁵, Susan Solomon¹

- 5
6 1. Department of Earth, Atmospheric and Planetary Sciences, Massachusetts Institute of
7 Technology, Cambridge, MA 02139, USA
8 2. NOAA Chemical Sciences Laboratory (CSL), Boulder, CO 80305-3328, USA
9 3. NASA Goddard Space Flight Center, Greenbelt, MD, USA
10 4. Science Systems and Applications, Inc., Lanham, MD, USA
11 5. Laboratory for Air Pollution/Environmental Technology, Empa, Swiss Federal
12 Laboratories for Materials Science and Technologies, Duebendorf, Switzerland
13

14 *Correspondence to:* Megan Lickley (mllickley@mit.edu)
15

16 **Abstract**

17 Halocarbons contained in equipment such as air conditioners, fire extinguishers, and foams
18 continue to be emitted after production has ceased. These ‘banks’ within equipment and
19 applications are thus potential sources of future emissions, and must be carefully accounted for
20 in order to differentiate nascent and potentially illegal production from legal banked emissions.
21 Here, we build on a probabilistic Bayesian model, previously developed to quantify CFC-11, 12
22 and 113 banks and their emissions. We extend this model to a suite of banked chemicals
23 regulated under the Montreal Protocol (HCFC-22, HCFC-141b, and HCFC-142b, halon 1211,
24 and halon 1301, and CFC-114 and CFC-115) along with CFC-11, 12 and 113 in order to quantify
25 a fuller range of ozone-depleting substance banks by chemical and equipment type. We show
26 that if atmospheric lifetime and prior assumptions are accurate, banks are very likely larger than
27 previous international assessments suggest, and that total production has been very likely higher
28 than reported. We identify that banks of greatest climate-relevance, as determined by global
29 warming potential weighting, are largely concentrated in CFC-11 foams and CFC-12 and HCFC-
30 22 non-hermetic refrigeration. Halons, CFC-11, and 12 banks dominate the banks weighted by
31 ozone depletion potential. Thus, we identify and quantify the uncertainties in substantial banks
32 whose future emissions will contribute to future global warming and delay ozone hole recovery
33 if left unrecovered.
34

35 **1. Introduction**
36

37 The Montreal Protocol regulates the production of ozone-depleting substances (ODPs), and its
38 implementation has avoided a world with catastrophic stratospheric ozone depletion (Newman et
39 al., 2009). Globally, there has been a near-cessation of chlorofluorocarbon (CFC) and halon
40 production since 2010, and global production of the replacement hydrochlorofluorocarbons
41 (HCFCs), are scheduled to be phased-out by 2030. Despite production phase-out, these
42 chemicals persist in old equipment produced prior to phase-out, such as refrigeration, air
43 conditioners, foams, and fire extinguishers. These reservoirs of materials (termed ‘banks’)
44 continue to be sources of emissions (e.g., Carpenter and Daniel et al., 2018). Previously
45 published estimates of bank sizes and bank emissions vary widely due to different estimation
46 techniques that incorporate incomplete or imprecise information (Kuijpers & Verdonik et al.,
47 2009; Montzka & Fraser et al., 2003). This uncertainty obscures ongoing emissions attribution
48 and undermines international efforts to evaluate global compliance with the Montreal Protocol.

- Deleted: evaluate
- Deleted: ongoing compliance with the Montreal Protocol
- Deleted: versus
- Deleted: the
- Deleted: the major
- Deleted: -
- Deleted: ,
- Deleted: -

- Deleted: .
- Deleted: (Kuijpers & Verdonik, 2009; WMO, 2003)

59 In earlier work, [Lickley et al. \(2020, 2021\)](#) developed a Bayesian probabilistic banks model for
60 CFCs that incorporates the widest range of constraints to date (Lickley et al., 2020, 2021). Here,
61 we extend this model to the suite of major chemicals regulated by the Protocol that are subject to
62 banking.

63 Previously published assessments typically rely on one of three modeling approaches to
64 estimate bank sizes and to then estimate emissions associated with these banks. In the “top-
65 down” approach (e.g. [Montzka & Fraser et al., 2003](#)), banks are estimated as the cumulative
66 difference between reported production and observationally-derived emissions. However, by
67 taking the cumulative sum of a small difference between two large values, small biases in
68 emissions or reported production estimates can propagate into large biases in bank estimates
69 (Velders & Daniel, 2014). Some type of bias is thus expected since total production has very
70 likely been greater than reported production both due to under-reporting of production (e.g.
71 [Gamlen et al., 1986](#); [Montzka et al., 2018](#)) and due to the exclusion of point-of-production losses
72 in reported production values. Further, emissions estimates rely on observed concentrations
73 along with global lifetime estimates, which have large uncertainties associated with them (M. Ko
74 et al., 2013).

75 The second approach relies on a “bottom-up” accounting method ([Ashford et al., 2004](#);
76 [Campbell & Shende et al., 2005](#)) where the inventory of sales by equipment type are carefully
77 tallied along with estimated release rates by application use. The bottom-up approach also relies
78 on sales data from surveys of various equipment types and products as well as estimates of their
79 respective leakage rates ([Campbell & Shende et al., 2005](#)). These are all subject to uncertainties,
80 which contribute to uncertainties in bottom-up bank estimates as well. A limitation of the
81 bottom-up method is that observed atmospheric concentrations are used only as a qualitative
82 check and are not explicitly accounted for in the analysis. Another important limitation is that
83 data used in the bottom-up accounting method are unobserved but rather rely on estimated
84 processes along with reported data, such as production or sales of equipment, thus any bias in
85 reporting could propagate into large biases in bank estimates.

86 The third approach, and the one used in more recent ozone assessments (WMO, 2011, 2014,
87 2018) uses a hybrid approach to calculate banks. Bottom-up banks estimated for 2008 are used
88 as the starting point of the calculations. These banks are taken from ([Campbell & Shende et al.,](#)
89 [2005](#)), and represent interpolated values from the 2002 and 2015 estimates. The banks are then
90 brought forward to the present time by adding the cumulative reported production and subtracting
91 the cumulative observationally-derived emission from 2008 through the present. This approach is
92 consistent with 2008 bottom-up bank estimates by design, however, as time between 2008 and
93 the present has grown, the cumulative errors associated with the top-down approach become
94 larger.

95 The modeling approach applied in the present study relies on Bayesian inference of banks
96 ([Lickley et al., 2020, 2021](#)) where banks are estimated using an approach called Bayesian
97 parameter estimation. In this approach a simulation model of the bottom-up method is
98 developed, where prior distributions of input parameters are constructed from previously
99 published values, accounting for large uncertainties in production and bank release rates. The
100 simulation model simultaneously models banks, emissions, and atmospheric concentrations.
101 Parameters in the simulation model are then conditioned (or updated) on observed concentrations
102 by applying Bayes’ theorem. The final result is a posterior distribution of banks by chemical and
103 equipment type, along with an updated estimate of production and release rates for each
104 equipment type. This approach incorporates data and assumptions from both the bottom-up and
105 top-down approaches, providing a simulation model consistent with the bottom-up accounting
106 approach while also being consistent with observed concentrations within their uncertainties.

Deleted: we developed

Deleted: (e.g. WMO, 2003)

Deleted: under-

Deleted: to some extent

Deleted:

Deleted:

Deleted: ,

Deleted: and

Deleted: (SPARC, 2013)

Field Code Changed

Deleted: 2006

Deleted: (Ashford et al., 2004; IPCC/TEAP, 2006),

Deleted: (SROC, 2005)

Deleted: s

Deleted: SROC (2006)

Deleted: y

122 The remainder of the paper includes the following: Section 2 presents the Bayesian modeling
123 approach along with data used in the analysis. Section 3 provides a summary of the results of
124 our analysis for each of the chemicals considered here. Finally, Section 4 provides a discussion
125 of our primary findings and limitations of the analysis.

127 2. Methods

128
129 The Bayesian modeling approach from Lickley et al. (2020, 2021) draws on a Bayesian analysis
130 approach called Bayesian melding, designed by Poole & Raftery (2000), that allows us to apply
131 inference to a deterministic simulation model. We employ a version of this method that we
132 henceforth refer to as Bayesian Parameter Estimation (BPE), which allows for input parameter
133 uncertainty (Bates et al., 2003; Hong et al., 2005). The model flow is implemented as follows;
134 first we develop a deterministic simulation model, representing the “bottom-up” accounting
135 method that simultaneously simulates banks, emissions, and mole fractions for each chemical
136 and equipment type. In this analysis, the chemicals considered include CFC-11, 12, 113, 114,
137 and 115, HCFC-22, 141b, and 142b, and halon, 1201, and 1311. Prior distributions for each of
138 the input parameters are based on previously published estimates. We then specify the
139 likelihood function as a function of the difference between observed and simulated mole
140 fractions. Finally, we estimate posterior distributions of both the input and output parameters by
141 implementing Bayes’ Rule using a sampling procedure. Each of the steps of the BPE are
142 described in more detail below.

144 2.1 Simulation Model

145 The simulation model is comprised of equations (1) – (5) which simultaneously models banks,
146 emissions, and mole fractions for each chemical by equipment type for all years with available
147 data up until 2019. Starting dates differ by chemical, see the Supplement for details. The
148 simulation model is specified as follows;

$$150 B_{j,t+1} = (1 - RF_{j,t}) \times B_{j,t} + (1 - DE_{j,t}) \times P_{j,t} \quad (1)$$

151 where $B_{j,t}$, is banks and $P_{j,t}$ is production of equipment category, j , in year, t . $RF_{j,t}$ reflects the
152 fraction of the bank released and $DE_{j,t}$ reflects the fraction of production that is directly emitted
153 in equipment category, j , year, t . These same parameters are used to simulate emissions, $E_{j,t}$:

$$156 E_{j,t+1} = RF_{j,t} \times B_{j,t} + DE_{j,t} \times P_{j,t} \quad (2)$$

157 Total banks, $B_{\text{Total},t}$, and total emissions, $E_{\text{Total},t}$, are then estimated as the sum across all N
158 equipment categories;

$$161 B_{\text{Total},t} = \sum_{j=1}^N B_{j,t} \quad (3)$$

$$163 E_{\text{Total},t} = \sum_{j=1}^N E_{j,t} \quad (4)$$

164 For chemicals where feedstock usage is reported, an additional term in eq (4) is included that
165 accounts for feedstock emissions. Emissions, along with an assumed atmospheric lifetime, τ_t ,
166 taken as the SPARC (2013) multi-model time-varying mean are then used to simulate
167 atmospheric mole fractions, MF_t ;

Deleted: -

Deleted: are then used to simulate atmospheric mole fractions, MF_t

172

$$MF_{t+1} = \exp\left(\frac{-1}{\tau_t}\right) \times MF_t + A \times E_{\text{Total},t} \quad (5)$$

174

175 where A is a constant that converts units of emissions **by mass** to units of mole fractions, **and**
 176 **also takes into account a fixed factor of 1.07 taken from Daniel et al. (2007) that accounts for the**
 177 **discrepancy between surface mole fraction concentrations and the global mean value.**

178

179

180 2.2 Prior Distributions

181 **The input parameters in the simulation model described above require initial values to be**
 182 **assigned, along with their probability distributions. These prior distributions ('priors') are**
 183 developed to estimate mole fractions, emissions, and banks for CFC-11, 12, 113, 114, and 115,
 184 HCFC-22, 141b, and 142b, and halon 1201 and 1311. Categories of bank equipment are defined
 185 by the categorization provided by AFEAS (2001), which varies by compound (shown in Table
 186 1). For halons, there is a single category of bank (fire extinguishing agent).

187 AFEAS data reports global annual production up to 2001, categorized by equipment type,
 188 which is generally **grouped as short, medium and long-term banks**. We use AFEAS data and
 189 categorization to develop our production priors and adopt the WMO (2003) correction where
 190 AFEAS production values are used up until 1989 and then scaled to match UNEP global
 191 production values for all years following 1989. After AFEAS data ends, we assume the relative
 192 production in each category remains constant for all years following 2001. Uncertainty in
 193 production priors is assumed to follow a multivariate log-normal distribution, where temporal
 194 correlation in production reporting bias is estimated in the BPE. Prior distributions differ by
 195 chemical and are developed to be wide enough for atmospheric mole fraction priors to contain
 196 observations. See the Supplement for details on production priors for each chemical.

197 The emissions function by bank equipment type can be characterized by the fraction of
 198 production that is directly emitted during the year of production (DE) and the fraction of the
 199 bank that is emitted in each subsequent year. Prior estimates for emissions functions come from
 200 previously reported data and differ by chemical and equipment type (see the Supplement).
 201 Broadly speaking, it has been estimated that chemicals contained in short-term banks are fully
 202 emitted within the first two years after production, medium-term banks lose about 10 – 20% of
 203 their material each year, and long-term banks can lose as little as 2% of their material each year
 204 (Ashford et al., 2004). We use previously published estimates to develop emissions function
 205 priors specific to each chemical and bank type along with wide uncertainties, as specified in the
 206 Supplement.

207 Amounts of halocarbons used for feedstock production are available annually
 208 (UNEP/TEAP, 2021). A prior mean leakage rate of 2% was assumed during production, which
 209 reflects **an approximate average of values across** different facilities (MCTOC, 2019).

210

211 **Table 1:** Application type of halocarbon banks by chemical

Chemical	Short Bank	Medium Bank	Long Bank
CFC-11	Aerosols Open-cell foam	Non-hermetic refrigeration	Closed-cell foam
CFC-12	Aerosols Open-cell foam	Non-hermetic refrigeration	Refrigeration
CFC-113	solvents		Heat pump
CFC-114			Heat pump

Deleted: to

Deleted: !

Formatted: Highlight

Deleted: P

Deleted: for each of the input parameters in the simulation model described above

Deleted: -

Deleted: ,

Deleted: ers

Deleted: categorized

Deleted: into

Deleted: medium

Deleted: between

CFC-115	Propellant		Air conditioning
HCFC-22	Open-cell foam	Non-hermetic refrigeration	Foam
HCFC-141b	Open-cell foam	Non-hermetic refrigeration	Foam
HCFC-142b		Non-hermetic refrigeration	Foam
Halon-1211		Fire extinguishing agent	
Halon-1301		Fire extinguishing agent	

Deleted: ers

Deleted: extinguishers

224
225
226
227
228
229

2.3 Likelihood function

For each chemical, the likelihood function is a multivariate normal likelihood function of the difference between modeled and observed mole fractions;

$$P(D_{t1}, \dots, D_{tN} | \theta) = \frac{1}{(2\pi)^{\frac{N}{2}} \sqrt{|S|}} \exp \left\{ -\frac{1}{2} \Delta^T S^{-1} \Delta \right\} \quad (6)$$

231

232 Where D_{t1}, \dots, D_{tN} is yearly globally-averaged observed mole fractions for all years where
233 observations are available and θ represents that vector of input and output parameters from the
234 simulation model. Δ is an $N \times 1$ vector of the difference between yearly observed and modeled
235 mole fractions and is assumed to have a mean zero, and covariance function S . S therefore
236 represents the sum of uncertainties between observed and modeled mole fractions. While there
237 are published estimates of uncertainties in observed mole fractions, we do not know the
238 uncertainties in modeled mole fractions. Therefore, we estimate S separately for each chemical,
239 as is done in (Lickley et al., 2020). The off-diagonals in the covariance function incorporate a
240 correlation term, $\rho_{S_{ij}}$ which accounts for our assumption that there is high autocorrelation in the
241 bias between modeled and observed mole fractions. Correlation terms for each chemical are
242 reported in the Supplement along with prior estimates of the uncertainty parameters used for
243 diagonal elements in S . Each column and row in S is therefore populated as:

244

$$S_{i,j} = \sigma_i \sigma_j \rho_S^{|i-j|}$$

246 where σ_i and σ_j represent the sum of the uncertainties in observed and modeled mole fractions at
247 time i and j , respectively, and are inferred in the BPE, whereas ρ_S is prescribed.

248

249 Observations come from the Advanced Global Atmospheric Gas Experiment (AGAGE;
250 <https://agage.mit.edu>) data set (Prinn et al., 2000; Prinn et al., 2018), with the exception of CFC-
251 11 and 12 which, following Lickley et al. (2021), come from the AGAGE and the National
252 Oceanographic and Atmospheric Administration's (NOAA) merged data sets (Engel et al.,
253 2019). Data are aggregated into annual global mean mole fractions. The time frame of
254 availability of observations differs by chemical (see the Supplement).

255

2.4 Posterior Distributions

Following Bayes' Rule, we specify our posterior distribution as;

258

$$P(\theta | D_{t1}, \dots, D_{tN}) = \frac{P(\theta) P(D_{t1}, \dots, D_{tN} | \theta)}{P(D_{t1}, \dots, D_{tN})} \quad (7)$$

260

261 Where $P(\theta)$ represents the joint prior distribution of the input and output parameters described
262 in the simulation model in Section 2.1.

Deleted: do not

Deleted: ,

Deleted: t

268
269 The analytical form of the posterior distribution is intractable. Thus, we estimate the posterior
270 using a sampling procedure (the sampling importance resampling (SIR) method) to estimate the
271 marginal posterior distributions (Bates et al., 2003; Hong et al., 2005; Rubin, 1988). To
272 implement SIR we draw 1,000,000 samples from the priors, run the simulation model, and then
273 resample from the priors 100,000 times using an importance ratio, which is proportional to the
274 likelihood function. These sample sizes were chosen such that multiple iterations of the model
275 produce consistent results.
276

277 3. Results

278 Figure 1 shows observed globally averaged mole fractions compared to BPE estimated mole
279 fractions for each chemical. Figure 2 shows BPE estimated and observationally-derived
280 emissions, assuming the SPARC time-varying multi-model mean lifetime for each species.
281 Posterior estimates agree well with observations for the majority of time periods and chemicals.
282 Note, however, that BPE estimates from Lickley et al. (2021) match observed and
283 observationally-derived estimates more closely for CFC-11 than they do in the present analysis.
284 We attribute this difference in consistency to atmospheric lifetimes being assumed in the present
285 analysis, whereas they were inferred in Lickley et al. (2021), which found inferred lifetimes to be
286 somewhat shorter than the SPARC multi-model mean values. Shorter lifetimes would allow
287 modeled mole fractions to decline more quickly following 1990, better matching observations. A
288 notable discrepancy occurs for CFC-115, where modeled mole fractions are increasing
289 throughout the entire simulation period, whereas observed mole fractions from 2000 onwards are
290 relatively constant. This discrepancy could be explained by the large uncertainties in
291 atmospheric lifetimes of CFC-115 (Vollmer et al., 2018), if atmospheric lifetimes are in fact
292 substantially shorter than the SPARC multi-model mean.
293

294 Figure 3 provides a comparison of BPE bank estimates alongside previously published bank
295 estimates. BPE bank estimates are generally higher than other published values. This can be
296 explained by production uncertainties that are accounted for in the present analysis. Our analysis
297 suggests that production has very likely been underreported for nearly all chemicals. Table 2
298 provides a summary of our estimated bias in cumulative reported production throughout the
299 simulation period for each chemical type. With the exception of CFC-113 and CFC-115, we find
300 our inferred cumulative production to be significantly higher than reported production (at the 1-
301 sigma level), with our median estimate suggesting that production was as little as 9% higher than
302 reported for CFC-12 and as high as 50% higher than reported for Halon₁₂₁₁. Note, however,
303 high uncertainties in lifetimes for Halon 1211 exist (Ko et al., 2013) and could explain part of
304 this discrepancy. We would expect any consistent bias in reported production to be a bias low,
305 since consistent undercounting of production is more plausible than overcounting production.
306 The exception for this would be the base year, which reduction targets are made with reference
307 to. In this instance, we would expect overreporting for this year to be more likely. Another
308 possible explanation for the discrepancy in production estimates is that total reported chemical
309 production under the UNEP does not account for leakage during chemical manufacturing, but
310 rather only leakage that occurs during the application of the chemical. To our knowledge, this
311 potential leakage during chemical manufacturing has not been well-documented or previously
312 quantified.
313
314

Deleted: -

Deleted: M.

Deleted: less unlikely

318 **Table 2:** Estimated bias in cumulative reported production. Values indicate the percent
 319 difference between inferred cumulative production from the onset of production to 2019 relative
 320 to reported production, for all uses except for feedstock production. Positive values indicate the
 321 percent by which inferred production is higher than reported.

Chemical Name	CFC-11	CFC-12	CFC-113	CFC-114	CFC-115
Median percentage inferred bias (16th, 84th percentile)	12% (9%, 13%)	9% (7%, 11%)	-1% (-3%, 0%)	11% (9%, 13%)	-1% (-2%, 5%)
Median absolute inferred bias (16th, 84th percentile) [Gg]	1146 (900, 1291)	1208 (976, 1439)	-37 (-76, -3)	58 (46, 70)	-2 (-4, 11)
Chemical Name	HCFC-22	HCFC-141b	HCFC-142b	Halon_1211	Halon_1301
Median percentage inferred bias (16th, 84th percentile)	10% (6%, 13%)	12% (6%, 19%)	22% (17%, 28%)	50% (41%, 59%)	24% (18%, 32%)
Median absolute inferred bias (16th, 84th percentile) [Gg]	1249 (828, 1712)	315 (153, 511)	220 (166, 281)	137 (114, 164)	36 (26, 49)

Formatted: Superscript
 Formatted: Superscript
 Deleted: -
 Deleted: -

322
 323
 324 Figure 4 shows the breakdown of emissions by equipment type over time. For CFCs, emissions
 325 from short-term banks tend to peak around 1990, as spray applications were banned earlier than
 326 other applications, after which emissions from medium and long-term banks become more
 327 dominant emission sources. This is to be expected as the phase-out of production after 1990
 328 would lead to more CFC emissions from existing banks rather than new, short-lived equipment.
 329 For HCFC-22, most of the emission throughout the entire time period is from medium banks,
 330 which is largely non-hermetic refrigeration. Long banks (i.e. foams) dominate emissions for
 331 HCFC-141b and for HCFC-142b, where both foams and non-hermetic refrigeration are
 332 prominent emission sources throughout the simulation period. Estimated feedstock emissions
 333 averaged over 2010 – 2019 are shown in Table 3. HCFC-22 is the largest source of feedstock
 334 emissions by mass, but CFC-113 feedstock emissions are estimated to be larger when weighted
 335 by GWP100 and ODP.

Deleted: ,

336
 337 **Table 3:** Estimated feedstock emissions averaged from 2010 – 2019 from the Bayesian analysis.
 338 Emissions are weighted by mass, global warming potential (GWP100) relative to CO2 over a
 339 100-year time horizon for a CO₂ concentration of 391ppm, and by ozone depletion potential
 340 (ODP) relative to CFC-11 (WMO, 2018).

Feedstock Emissions	CFC-113	HCFC-22	HCFC-142b
By mass	3.4 Gg/yr	9.3 Gg/yr	2.1 Gg/yr
By GWP100	20, 838 Gg/yr	16,591 Gg/yr	4,302Gg/yr
By ODP	2.8 Gg/yr	0.3 Gg/yr	0.1 Gg/yr

341
 342 Figure 5 shows the relative quantity of banked materials by chemical type. Banks are weighted
 343 by mass (Figure 5a), by global warming potential (GWP100; Figure 5b), and by ozone depleting
 344 potential (ODP; Figure 5c). Our best estimate is that the sum of the HCFCs currently comprise
 345 about 77% of banks by mass. However, in terms of climate impacts, CFC-11, 12 and HCFC-22
 346 are the largest banked materials weighted by GWP100, accounting for 36%, 14%, and 36% of

350 current banks, respectively. When banks are weighted by ODP, CFC-11 and 12 represent 46%
351 and halons also represent 46% of current banked chemicals.

352
353 Figure 6 shows the composition of banks by chemical type. This, together with Figure 5,
354 provides insight into the most prominent banked sources of halocarbons with regards to
355 GWP100 and ODP. In terms of GWP100, CFC-11 banks largely reside in foams, whereas CFC-
356 12 and HCFC-22 are largely in non-hermetic refrigeration; the latter may be more readily
357 recoverable. In terms of ODP, CFC-11 foams and CFC-12 non-hermetic refrigeration remain
358 important, along with halons which are all contained in fire extinguishers, a recoverable
359 reservoir.

362 4. Discussion and Conclusions

363 This analysis suggests that if lifetime assumptions are correct, published bank estimates using
364 either the top-down or bottom-up methods were likely underestimating bank sizes for all banked
365 chemicals due to underreporting of production (see Table 2). The Bayesian approach used in this
366 analysis does not assume production is known precisely, but rather jointly infers production
367 along with the other parameters in the simulation model, providing probabilistic estimates of
368 historical production values. Previously published bank estimates (Ashford et al., 2004; Kuijpers
369 & Verdonik, 2009; Montzka and Fraser et al., 2003) do not infer production, but rather assume it
370 is known, or consider different scenarios. We argue that production assumptions have been
371 biased low due to underreporting of total production and potentially unaccounted for leakage
372 during chemical manufacturing and thus have led to published bank estimates that were also
373 biased low.

374
375 Discrepancies between observed mole fractions and BPE-derived mole fractions are notable for
376 the suite of chemicals considered here. While the majority fall within the 90% confidence
377 interval throughout most of the time periods, the trends in concentrations between observations
378 and inferred mole fractions do not always agree. This discrepancy could be related to our
379 partitioning of production type following 2003 (i.e. after AFEAS data ends). Another important
380 limitation in this analysis is in the treatment of atmospheric lifetimes, which could also explain
381 some of these discrepancies. The present analysis assumes atmospheric lifetimes are known and
382 equal to the SPARC (2013) time varying multi-model mean lifetimes. However, previous work
383 has indicated potential biases in SPARC lifetimes, for example for CFCs (Lickley et al., 2021).
384 The potential bias in atmospheric lifetimes would result in biased bank estimates in the present
385 manuscript and requires further analysis.

386
387 This modeling approach makes no assumptions about end-of-life emissions. Certain bank
388 estimates assume that applications are dismantled at the end of their lifetime, which would both
389 contribute to decreased banks and increased emissions at fixed years after production (e.g.
390 (UNEP/TEAP, 2019). We do not make this assumption as we believe it would be more realistic
391 for dismantling of equipment to occur over a range of years after production, which would
392 effectively be captured by our bank release fraction estimate. We do, however, test the
393 sensitivity of our bank estimate to end-of-life (EOL) emissions occurring in a single year after
394 production. This we term the EOL scenario and test the sensitivity of banks for CFC-11, CFC-
395 12 and HCFC-22, the three largest banks by global warming potential. The modeling approach
396 is described in the SM and results are shown in Figure SM1. Perhaps unexpectedly, CFC-11
397 posterior bank estimates are ~25% higher in 2020 in the EOL scenario relative to the scenario

Field Code Changed

Field Code Changed

398 described in the main text. However, banks in the EOL scenario are decreasing faster than those
399 described in the main text. The larger bank size is due to posterior bank release fractions being ~
400 2% for the EOL scenario relative to 3% for the scenario described in the main text. The faster
401 depletion of the banks in 2020 can be explained by the addition of the EOL decommissioning
402 parameter. These larger bank estimates reflect the consistency of the Bayesian modeling
403 approach where all parameters are jointly inferred. Including an additional process in the model
404 requires that multiple parameters be updated to be consistent with observations. For CFC-12, the
405 EOL scenario produces significantly smaller banks from about 1990 onwards, however, the
406 emissions profile has an artificial dip in emissions relative to observationally-derived emissions,
407 suggesting a set year for decommissioning is not a realistic modeling assumption. For HCFC-22
408 banks are not substantially different between the two scenarios.
409

410 There are important discrepancies between CFC-113 feedstock emissions inferred here and those
411 estimated in the previous analysis (Lickley et al., 2020). In Lickley et al. (2020), feedstock
412 emissions were assumed to be the difference between observationally-derived emissions and
413 inferred bank emissions. In the present analysis, prior distributions of feedstock production and
414 leakage rates are developed and feedstock emissions are then inferred. In the present analysis,
415 observationally-derived CFC-113 emissions are higher than total BPE inferred emissions at the
416 1-sigma level from 2010 onwards. This suggests that either observationally-derived emissions
417 are too high, or our BPE estimates are too low. In Lickley et al. (2021), we find that atmospheric
418 lifetimes of CFC-113 are very likely lower than the SPARC multi-model time varying mean,
419 used in the present analysis. This would imply that the observationally-derived emissions shown
420 in Figure 2 are biased low, suggesting an even larger discrepancy between BPE inferred total
421 emissions and observationally derived emissions. Therefore, it seems plausible that the
422 discrepancy is due to prior feedstock emissions estimates being biased low due to larger leakage,
423 or CFC-113 is being produced for a use that is not allowed under the Montreal Protocol.
424

425 Finally, some important details about production and destruction were not fully accounted for in
426 this analysis. For one, feedstock priors were only included for CFC-113, HCFC-22, and HCFC-
427 142b, which could be limiting our assessment of the sources of emissions for other chemicals.
428 However, published feedstock values for other chemicals are not available and leakage rates in
429 feedstock applications may be uncertain. In addition, we do not account for non-dispersive
430 production in our analysis, namely the production of chemicals as by-products. It is possible, for
431 example, that some of the discrepancies in CFC-115 emissions could be explained by non-
432 dispersive emissions as identified by Vollmer et al., (2018). Further, we do not consider end-of-
433 life destruction of equipment as there are no published records, to our knowledge, of these
434 processes. Finally, we were not able to account for a more detailed breakdown in production by
435 equipment type than what has been published by AFEAS, which discretizes production into, at
436 most, four categories of equipment, and does not provide data beyond 2003. Without publicly
437 available details of these processes, modeling of banks and emissions will continue to be limited.
438

439 **Code Availability:** All analyses were done in MATLAB. All code used in this work is available
440 at <https://github.com/meglickley/HalocarbonBanks>
441

442 **Data Availability:** The datasets generated and/or analyzed during the current study are available
443 at <https://github.com/meglickley/HalocarbonBanks>
444

Field Code Changed

Deleted: (

446 **Author Contributions.** All authors contributed to the conceptualization of the manuscript.
447 M.L. conducted the analysis. M.L. prepared the manuscript with contributions from all authors.

448
449 **Competing Interests.** The authors declare that they have no conflict of interest.

450
451 **Acknowledgements.** M.L. and S.S. gratefully acknowledge the support of VoLo foundation
452 and grant 2128617 from the atmospheric chemistry division of NSF. AGAGE is supported
453 principally by NASA (USA) grants to MIT and SIO, and also by: BEIS (UK) and NOAA (USA)
454 grants to Bristol University; CSIRO and BoM (Australia); FOEN grants to Empa (Switzerland);
455 NILU (Norway); SNU (Korea); CMA (China); NIES (Japan); and Urbino University (Italy). [E.F.](#)
456 [acknowledges support of the NASA Headquarters Atmospheric Composition Modeling and](#)
457 [Analysis Program.](#)

458 459 460 **References**

- 461 AFEAS. (2001). AFEAS 2001 database. Retrieved from
462 [https://unfccc.int/files/methods/other_methodological_issues/interactions_with_ozone_layer](https://unfccc.int/files/methods/other_methodological_issues/interactions_with_ozone_layer/application/pdf/cfc1100.pdf)
463 [/application/pdf/cfc1100.pdf](https://unfccc.int/files/methods/other_methodological_issues/interactions_with_ozone_layer/application/pdf/cfc1100.pdf)
- 464 Ashford, P., Clodic, D., McCulloch, A., & Kuijpers, L. (2004). Emission profiles from the foam
465 and refrigeration sectors comparison with atmospheric concentrations. Part 1: Methodology
466 and data. *International Journal of Refrigeration*, 27(7), 687–700.
- 467 Bates, S. C., Cullen, A., & Raftery, A. E. (2003). Bayesian uncertainty assessment in
468 multicompartment deterministic simulation models for environmental risk assessment.
469 *Environmetrics: The Official Journal of the International Environmetrics Society*, 14(4),
470 355–371.
- 471 Campbell, N., Shende, R., Bennett, M., Blinova, O., Derwent, R., McCulloch, A., et al. (2005).
472 HFCs and PFCs: Current and Future Supply, Demand and Emissions, plus Emissions of
473 CFCs, HCFCs and Halons. In B. Metz, L. Kuijpers, S. Solomon, S. O. Andersen, O.
474 Davidson, & J. Pons (Eds.), *IPCC/TEAP Special Report, Safeguarding the Ozone Layer and*
475 *the Global Climate System: Issues Related to Hydrofluorocarbons and Perfluorocarbons*.
476 WMO.
- 477 Carpenter, L. J., Daniel, J. S., Fleming, E. L., Hanaoka, T., Hu, J., Ravishankara, A. R., et al.
478 (2018). Scenarios and Information for Policy Makers. In *Depletion: 2018, Global Ozone*
479 *Research and Monitoring Project—Report No. 58*. Geneva, Switzerland: World
480 Meteorological Organization.
- 481 Engel, A., Rigby, M., Burkholder, J. B., Fernandez, R. P., Froidevaux, L., Hall, B. D., et al.
482 (2019). *Update on Ozone-Depleting Substances (ODSs) and other gases of interest to the*
483 *Montreal Protocol, Chapter 1 in Scientific Assessment of Ozone Depletion: 2018, Global*
484 *Ozone Research and Monitoring Project - Report No. 58*. Geneva, Switzerland: World
485 Meteorological Organization.
- 486 Gamlen, P. H., Lane, B. C., Midgley, P. M., & Steed, J. M. (1986). The production and release to
487 the atmosphere of CCl₃F and CCl₂F₂ (chlorofluorocarbons CFC11 and CFC 12).
488 *Atmospheric Environment*, 20(6), 1077–1085.
- 489 Hong, B., Strawderman, R. L., Swaney, D. P., & Weinstein, D. A. (2005). Bayesian estimation
490 of input parameters of a nitrogen cycle model applied to a forested reference watershed,
491 Hubbard Brook Watershed Six. *Water Resources Research*, 41(3).
- 492 Ko, M., Newman, P., Reimann, S., & Strahan, S. (2013). Recommended Values for Steady-State
493 Lifetime. In M. K. W. Ko, P. A. Newman, S. Reimann, & S. E. Strahan (Eds.), *SPARC*

494 *Report on the Lifetimes of Stratospheric Ozone-Depleting Substances, Their Replacements,*
495 *and Related Species.*

496 Kuijpers, L. J. M., & Verdonik, D. (2009). *TEAP (Technology and Economic Assessment Panel),*
497 *Task Force Decision XX/8 Report, Assessment of Alternatives to HCFCs and HFCs and*
498 *Update of the TEAP 2005 Supplement Report Data.* Nairobi, Kenya. Retrieved from
499 [http://ozone.unep.org/teap/Reports/TEAP_0AReports/teap-may-2009-decisionXX-8-task-](http://ozone.unep.org/teap/Reports/TEAP_0AReports/teap-may-2009-decisionXX-8-task-forcereport.0A.pdf)
500 [forcereport.0A.pdf](http://ozone.unep.org/teap/Reports/TEAP_0AReports/teap-may-2009-decisionXX-8-task-forcereport.0A.pdf)

501 Lickley, M., Solomon, S., Fletcher, S., Rigby, M., Velders, G. J. M., Daniel, J., et al. (2020).
502 Quantifying contributions of chlorofluorocarbon banks to emissions and impacts on the
503 ozone layer and climate. *Nature Communications*, *11*(1380).
504 <https://doi.org/10.1038/s41467-020-15162-7>

505 Lickley, M., Fletcher, S., Rigby, M., & Solomon, S. (2021). Joint Inference of CFC lifetimes and
506 banks suggests previously unidentified emissions. *Nature Communications*, *12*(2920), 1–10.
507 <https://doi.org/https://doi.org/10.1038/s41467-021-23229-2> |

508 MCTOC. (2019). *Medical and Chemical Technical Options Committee, 2018 assessment.*
509 Retrieved from [https://ozone.unep.org/sites/default/files/2019-04/MCTOC-Assessment-](https://ozone.unep.org/sites/default/files/2019-04/MCTOC-Assessment-Report-2018.pdf)
510 [Report-2018.pdf](https://ozone.unep.org/sites/default/files/2019-04/MCTOC-Assessment-Report-2018.pdf)

511 Montzka, S. A., Fraser, P. J., Butler, J. H., Connell, P. S., Cunnold, D. M., Daniel, J. S., et al.
512 (2003). Controlled Substances and Other Source Gases. In *Scientific Assessment of Ozone*
513 *Depletion: 2002*. Geneva, Switzerland.

514 Montzka, S. A., Dutton, G. S., Yu, P., Ray, E., Portmann, R. W., Daniel, J. S., et al. (2018). An
515 unexpected and persistent increase in global emissions of ozone-depleting CFC-11. *Nature*,
516 *557*(7705), 413.

517 Newman, P. A., Oman, L. D., Douglass, A. R., Fleming, E. L., Frith, S. M., Hurwitz, M. M., &
518 Kawa, S. R. (2009). What would have happened to the ozone layer if chlorofluorocarbons
519 (CFCs) had not been regulated? *Atmospheric Chemistry and Physics*, *9*(6), 2113–2128.

520 Poole, D., & Raftery, A. E. (2000). Inference for deterministic simulation models: the Bayesian
521 melding approach. *Journal of the American Statistical Association*, *95*(452), 1244–1255.

522 Prinn, R. G., Weiss, R. F., Fraser, P. J., Simmonds, P. G., Cunnold, D. M., Alyea, F. N., et al.
523 (2000). A history of chemically and radiatively important gases in air deduced from
524 ALE/GAGE/AGAGE. *Journal of Geophysical Research Atmospheres*, *105*(D14), 17751–
525 17792. <https://doi.org/10.1029/2000JD900141>

526 Prinn, Ronald G., Weiss, R. F., Arduini, J., Arnold, T., Langley Dewitt, H., Fraser, P. J., et al.
527 (2018). History of chemically and radiatively important atmospheric gases from the
528 Advanced Global Atmospheric Gases Experiment (AGAGE). *Earth System Science Data*,
529 *10*(2), 985–1018. <https://doi.org/10.5194/essd-10-985-2018>

530 Rubin, D. B. (1988). Using the SIR algorithm to simulate posterior distributions (with
531 discussion). *Bayesian Statistics*, *3*, 395–402.

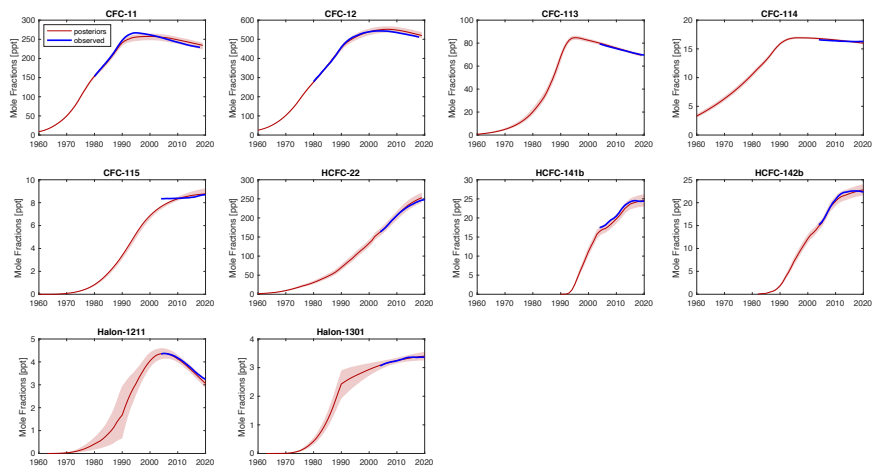
532 UNEP/TEAP. (2021). *TEAP Progress Report Volume 1*. Nairobi, Kenya. Retrieved from
533 <https://ozone.unep.org/system/files/documents/TEAP-2021-Progress-report.pdf>

534 UNEP. (2019). *Decision XXX/3 TEAP Task Force Report on unexpected emissions of*
535 *Trichlorofluoromethane (CFC-11) - Final Report (Volume 1)*. Nairobi, Kenya.

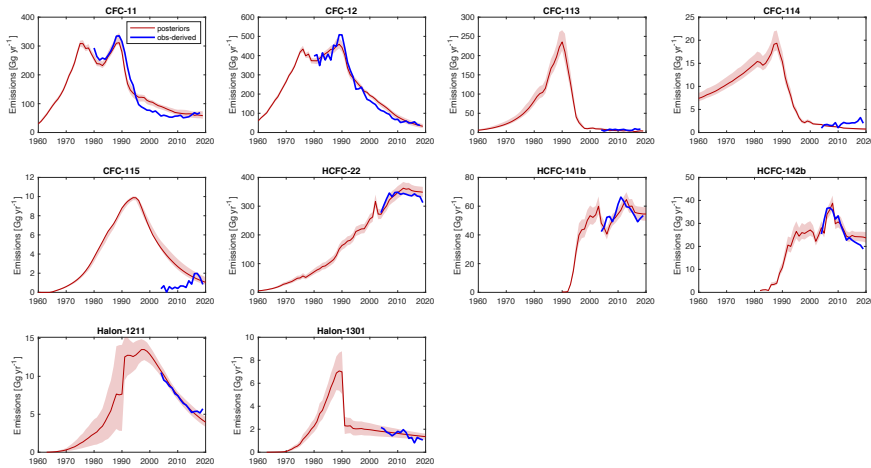
536 Velders, G. J. M., & Daniel, J. S. (2014). Uncertainty analysis of projections of ozone depleting
537 substances: mixing ratios, EESC, ODPs, and GWPs. *Atmospheric Chemistry and Physics*,
538 *14*(6), 2757–2776.

539 Vollmer, M. K., Young, D., Trudinger, C. M., Mühle, J., Henne, S., Rigby, M., et al. (2018).
540 Atmospheric histories and emissions of chlorofluorocarbons CFC-13 (CClF₃), Σ CFC-114
541 (C₂Cl₂F₄), and CFC-115 (C₂ClF₅). *Atmospheric Chemistry and Physics*, *18*(2), 979–1002.

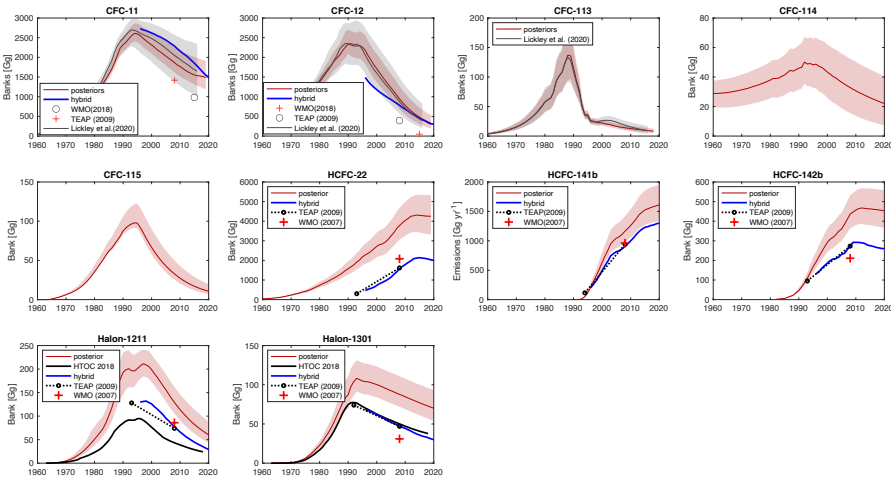
542 <https://doi.org/10.5194/acp-18-979-2018>
 543 WMO. (2003). WMO: Scientific Assessment of Ozone Depletion: 2002, Global Ozone Research
 544 and Monitoring Project – Report No. 47. Geneva, Switzerland: World Meteorological
 545 Organization (WMO),.
 546 WMO. (2011). *Scientific Assessment of Ozone Depletion: 2010, Global Ozone Research and*
 547 *Monitoring Project-Report No. 52.* Geneva, Switzerland.
 548 WMO. (2014). *Scientific Assessment of Ozone Depletion: 2014, World Meteorological*
 549 *Organization, Global Ozone Research and Monitoring Project-Report No. 55.* Geneva,
 550 Switzerland.
 551 WMO. (2018). WMO: Scientific Assessment of Ozone Depletion: 2018, Global Ozone Research
 552 and Monitoring Project – Report No. 58. Geneva, Switzerland: World Meteorological
 553 Organization (WMO),.
 554
 555
 556



557
 558 **Figure 1:** Modeled mole fractions versus observed mole fractions. Red lines indicate the
 559 posterior median mole fraction estimate from the Bayesian analysis (BPE), with shaded regions
 560 indicating the 90% confidence interval. Blue line indicates globally-averaged observed mole
 561 fractions.
 562

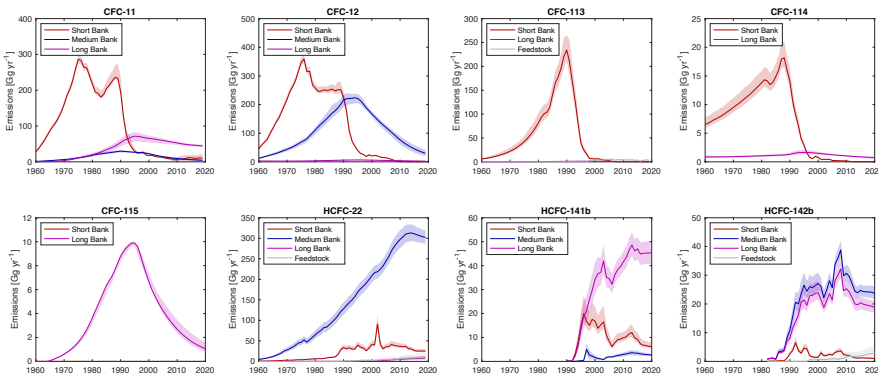


563
 564 **Figure 2:** Modeled emissions versus observationally-derived emissions. Red lines indicate the
 565 posterior median emissions estimate from the Bayesian analysis (BPE), with shaded regions
 566 indicating the 90% confidence interval. Blue line indicates observationally-derived emissions
 567 assuming the SPARC multi-model mean time-varying lifetimes.
 568
 569

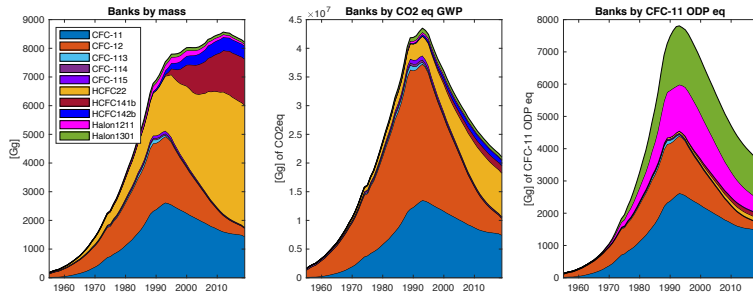


570
 571 **Figure 3:** Magnitudes of Bank estimates. The red line indicates the median posterior estimate of
 572 Banks from the Bayesian analysis, with shading indicating the 90% confidence interval.
 573 Previously published bank estimates are provided for comparison from TEAP (2009), WMO

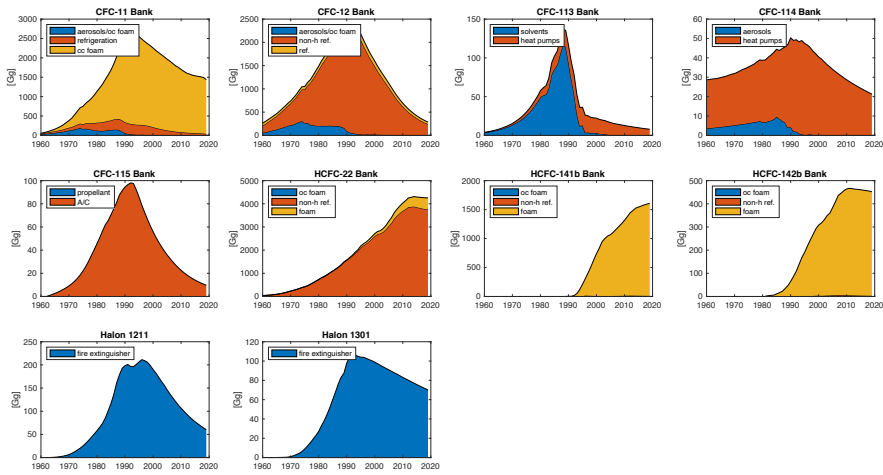
574 (2007), and WMO (2018), along with the hybrid approach updated to current estimated starting
 575 values.
 576



577
 578 **Figure 4:** Emissions by Source. Emissions estimates by various equipment types, summarized
 579 in Table 1, are shown here along with estimated emissions from feedstock usage. Lines indicate
 580 the median estimate, with the shaded region indicating the 90% confidence interval. Halons are
 581 not included in this figure as 100% of halon emissions come from the same application and are
 582 thus identical to Figure 2 halon totals.
 583



584
 585 **Figure 5:** Total banks by mass, global warming potential (GWP100; WMO, 2018) and ozone
 586 depleting potential (ODP; WMO, 2018). Bank estimates reported in the above figures are the
 587 median estimates from the Bayesian analysis.
 588



589
590
591
592
593
594

Figure 6: Bank size by equipment type. Bank estimates reported in the above figures are the median estimates from the Bayesian analysis. In the above legends, cc refers to closed-cell foams, non-h ref. refers to non-hermetic refrigeration, ref. refers to refrigeration, and A/C refers to air conditioning.